^{13}C CP/MAS NMR Chemical Shift and Molecular Dynamics Study of Charge-Transfer Interactions in Blends of Poly(2-[(3,5-dinitrobenzoyl)oxy]ethyl methacrylate) with Poly[(*N*-ethylcarbazol-3-yl)methyl methacrylate or acrylate]

Alexandra Simmons and Almeria Natansohn*

Department of Chemistry, Queen's University, Kingston, Ontario, Canada K7L 3N6

Received January 22, 1992

ABSTRACT: ^{13}C CP/MAS NMR was used to study charge-transfer interactions in the solid state in blends of a polyacceptor, poly[2-[(3,5-dinitrobenzoyl)oxy]ethyl methacrylate] (pDNBEM), with a polydonor, poly-[(*N*-ethylcarbazol-3-yl)methyl methacrylate or acrylate] (pNECMM or pNECMA). Upfield shifts were observed for aromatic carbons of pDNBEM in miscible blends, but not in two-phase blends, indicating a close approach of donor and acceptor groups in the miscible blends. $T_{1\rho}(C)$ was measured for all resolvable carbons in pDNBEM, pNECMA, and pNECMM between 40 and 90 °C. Variable-temperature studies confirmed the usefulness of $T_{1\rho}(C)$ as a motional parameter in these samples. All carbons except the α-CH_3 are on the low-temperature side of the $T_{1\rho}(C)$ minimum in the temperature range studied. Different types of motion contribute to relaxation of carbons in the main chain and in pendant groups. Pendant aromatic groups have some mode of sub-T_g motion, which increases smoothly in frequency or amplitude as the temperature is increased. Both types of carbons undergo a rapid increase in relaxation rate near T_g. No large changes in mobility were observed on blending pDNBEM with pNECMA or pNECMA, but in blends there appears to be some damping of motion at the same aromatic sites of pDNBEM where chemical shift changes were observed. These small motional changes do not account for the decrease in $T_{1\rho}(H)$ upon blending previously reported, confirming out interpretation of $T_{1\rho}(H)$ as a measure of interproton distance in these samples.

Introduction

It is becoming increasingly clear that the macroscopic properties of bulk polymers are related to their molecular-level structure and dynamics. In the solid state, both structure and dynamics are, to a large extent, determined by inter- and intramolecular interactions. These interactions may range from weak, such as van der Waals forces, to extremely strong, as in ion–ion interactions. One of our aims has been to gain a better understanding of charge-transfer (CT) interactions in polymers. CT or electron donor–acceptor (EDA) interactions are relatively weak, yet they are responsible for self-organization in many macromolecular systems, including some biological ones.

We have been investigating homopolymers containing pendant electron-donor or -acceptor moieties, donor–acceptor (D–A) copolymers, and polydonor (pD)/polyacceptor (pA) blends. Either (*N*-ethylcarbazol-3-yl)-methyl methacrylate (NECMM)[1-3] or (*N*-ethylcarbazol-3-yl)methyl acrylate (NECMA)[4] was used as a donor group, while 2-[(3,5-dinitrobenzoyl)oxy]ethyl methacrylate (DNBEM) was used as the acceptor group. The study of EDA interactions in these copolymers and blends is simplified by the fact that all three homopolymers are amorphous and do not self-associate. Rodriguez-Parada and Percec[5] found that phase separation of miscible pNECMM/pDNBEM blends occurs when they are heated above 185 °C. Therefore, by use of the appropriate processing conditions, one- or two-phase blends of the same composition can be obtained.

Advances in instrumentation and experimental techniques, such as dipolar decoupling, magic-angle spinning, and cross-polarization, have made it possible to routinely acquire high-resolution ^{13}C NMR spectra of solid polymers. Information about structure and dynamics previously buried in broad featureless ^1H spectra is now available. One can take advantage of the large chemical shift dispersion of ^{13}C to resolve nuclei in different chemical environments and measure relaxation rates at each resolvable carbon because the low abundance of ^{13}C precludes averaging of relaxation rates by spin diffusion. The average ^1H relaxation times can also be measured through the decay of the ^{13}C signal with the appropriate pulse sequence.

^{13}C CP/MAS-DD NMR spectroscopy has obvious advantages over bulk measurements such as dynamic mechanical or thermal analysis in the study of molecular-level structure and dynamics of solid polymers. We have been evaluating its use as a probe of CT interactions in D–A copolymers and pD/pA blends by measuring the chemical shifts and the proton and carbon rotating-frame relaxation time constants, $T_{1\rho}(H)$ and $T_{1\rho}(C)$. The transfer of electron density from donor to acceptor units upon charge-transfer complex (CTC) formation is reflected in chemical shift changes such as peak splittings and chemical shift changes of up to 5 ppm in CTCs of small-molecule analogues of pNECMM and pDNBEM.[3] However, significant changes in the spectra of pNECMM, pNECMA, or pDNBEM were not detected in polymer blends.

In general, the observation of chemical shift changes resulting from intermolecular interactions in polymer blends by ^{13}C CP/MAS-DD NMR is difficult because the resonances are broad. A strong interaction may be required before any effect can be seen. For example, changes in the line shape of the carbonyl carbon of a polyimide due to hydrogen bonding in blends with poly(ether sulfone)[6] or poly(benzimidazole)[7] have been reported. Hydrogen bonding is also believed to be responsible for 2–3 ppm upfield shifts in blends of poly(vinyl alcohol) with poly(methacrylic acid)[8] and blends of poly-(4-vinylphenol) with poly(ethylene oxide)[9], poly(vinyl methyl ketone)[10], or poly(methyl acrylate or methacrylate).[11] Hydrogen bonding results in a change in line shape and chemical shift of the ring carbon resonances of cellulose or methylolcellulose in blends with poly(4-vinylpyridine).[12]

Since CT interactions are relatively weak, their effect in polymer blends is harder to detect by ^{13}C CP/MAS-DD NMR. The increased resolution in solution has made it possible to use proton[13] and carbon[14] chemical shifts to estimate the extent of complexation in, for example, D–A

0024-9297/92/2225-3881$03.00/0

copolymers. ^{13}C CP/MAS NMR has been used to investigate CT complexation in a polymer–small-molecule complex of poly(*N*-vinylcarbazole) with 2,4,7-trinitro-9-fluorenone or 2,4,5,7-tetranitro-9-fluorenone.[15] In this paper we present spectra of a pNECMA/pDNBEM blend which exhibit small but significant differences from those of the homopolymers.

$T_{1\rho}$(H) is a measure of the efficiency of spin diffusion in a sample. It measures the strength of the H–H dipolar interactions, which depend on interproton distance and the spectral density at the observation frequency. We have examined $T_{1\rho}$(H) in NECMM–DNBEM copolymers,[2] pNECMM/pDNBEM blends,[3] and copolymers and blends containing NECMA and DNBEM units.[4] In all cases, we observed a reduced $T_{1\rho}$(H) upon CTC formation and attributed the increased rate of spin diffusion to a reduced interproton distance due to a pulling together of donor and acceptor units. The $T_{1\rho}$(H) values of the homopolymers are sufficiently different that $T_{1\rho}$(H) can be used to probe miscibility in blend samples, a significant advantage for the pNECMA/pDNBEM pair which have the same T_g, and appear phase-separated by SEM.[16] A list of prior applications of $T_{1\rho}$(H) to probe blend miscibility appears in ref 3. Because ^{13}C is a dilute species, the values of $T_{1\rho}$(C) for different types of carbons are not averaged by spin diffusion. For rigid proton-rich samples such as highly crystalline polyethylene, rotating-frame relaxation of carbon is dominated by spin–spin processes.[17] Schaefer et al. have shown that for most glassy polymers at room temperature $T_{1\rho}$(C) is predominantly spin–lattice in character.[18] They showed this to be true for poly(methyl methacrylate),[19] polycarbonates,[18,19] poly(phenylene oxide),[19] polystyrenes,[19,20] polysulfones,[19] poly(vinyl chloride),[19] and poly(ethylene terephthalate),[21] and the usefulness of $T_{1\rho}$(C) as a motional parameter is now firmly established.

In principle, one should be able to measure $T_{1\rho}$(C) for each resolvable carbon and obtain an estimate of the spectral density in the mid-kilohertz range at each site. This is a very attractive proposition since this is thought to be the frequency range of long-range cooperative motions involved in T_g. In practice, the interpretation of $T_{1\rho}$(C) is complicated. ^{13}C rotating-frame relaxation data can seldom be fit by a single exponential; rather, there is often a large difference in the initial and final slopes of the ln intensity vs delay time curve. This probably reflects not only a distribution of correlation time for motion at one site, but also a number of noninterconverting dynamic environments for chemically or structurally equivalent carbons.[19] The extent of the $T_{1\rho}$(C) dispersion has been related to the involvement of a given site in cooperative motion, which may be interchain as well as intrachain. One approach to simplify the comparison of $T_{1\rho}$(C)'s has been to use the average value provided by the initial ln intensity vs delay time slope, designated $\langle T_{1\rho}(C)\rangle$.

In spite of limitations in its quantitative interpretation, $T_{1\rho}$(C) has proven useful, particularly in conjunction with other NMR parameters, in examining motion in bulk polymers. The effect of the soft phase on motion in the hard phase of thermoplastic elastomers containing poly(butylene terephthalate) has been investigated,[22] as have mobility changes during curing of glycol methacrylate networks.[23] $T_{1\rho}$(C) has been measured in liquid-crystalline poly(ester amides)[24] and blends of poly(vinylphenol) with poly(methyl acrylate or methacrylate),[11] and a variable-temperature study of $T_{1\rho}$(C) in aromatic polyamide networks and swollen gels has appeared.[25]

We chose $T_{1\rho}$(C) as a probe for motional changes upon blending pDNBEM with pNECMM or pNECMA for several reasons. Miscible pD/pA blends exhibit an elevated T_g with respect to the weighted average of the components, while after decomplexation, the T_g of each phase is close to that of the pure homopolymer.[1-5] In addition, an extension of the rubbery plateau has been observed in viscoelastic measurements of pD/pA blends.[26] These observations suggest that CTCs act as thermally reversible cross-links between pD and pA chains. Since these data imply restriction of low-frequency motion in blends, we felt that measurement of $T_{1\rho}$(C) might provide site-specific information about the effects of CTC formation in polymer blends. Preliminary results were reported;[27] the whole body of data we collected is presented and its interpretation discussed in this work.

Experimental Section

Monomers were synthesized as described in the literature. NECMA and NECMM were obtained by the reduction of *N*-ethyl-3-carbazole carboxaldehyde to (*N*-ethylcarbazol-3-yl)methanol, followed by reaction with acryloyl or methacryloyl chloride.[28] The addition of ethylene glycol to 3,5-dinitrobenzoic acid forms 2-[(3,5-dinitrobenzoyl)oxy]ethanol, which reacts with methacryloyl chloride to give DNBEM.[29]

Free-radical polymerization of 0.5 M solutions of the monomer in toluene for several days at 60 °C with AIBN present at a level of 1% based on monomer weight gave pNECMA, pNECMM, and pDNBEM. Polymers were isolated by two reprecipitations from THF into methanol and dried for several days in vacuo above 70 °C. Purity of monomers and precursors, as well as the absence of residual monomer in the homopolymers, was confirmed by ^1H NMR in $CDCl_3$ or DMSO-d_6. Blends were prepared by mixing 1% (w/v) solutions of the homopolymers in boiling THF and then precipitating into methanol. Blends were dried in the same conditions as homopolymers. A portion of each blend was heated in vacuo to 10 °C above the phase separation temperature for several minutes and then quenched into liquid nitrogen. These blends are referred to herein as "decomplexed".

Homopolymer molecular weights were determined by gel permeation chromatography of 0.2 wt % THF solutions. A Waters Associates liquid chromatograph equipped with a Model 440 UV absorbance detector and a Model R401 differential refractometer was employed with a flow rate of 1 mL/min. Peak molecular weights were obtained by comparing retention times in μStyragel columns to those of polystyrene standards.

Proton-decoupled solid-state ^{13}C NMR spectra were obtained at room temperature on a Bruker CXP-200 spectrometer operating at 50.307 MHz equipped with a Doty probe, using cross-polarization and magic-angle spinning. A 3.9-μs $\pi/2$ pulse, corresponding to a rotating-frame frequency of 64 kHz, was used. The cross-polarization time was 5 ms, and the delay between scans was 4 s. A total of 800–1024 scans were required for each sample. Dipolar-dephased spectra were obtained by inserting a 60-μs delay after the 5-ms contact time.[30] Adamantane was used as an external reference.

$T_{1\rho}$(C) was measured between 40 and 90 °C using a pulse sequence in which the proton field is turned off for a variable time.[18,19] Delay times were arranged randomly with respect to their length, rather than in increasing order, to minimize any artifacts due to changes in temperature, magic-angle spinning, or other variables during the course of the experiment. Delay times varied from 0.2 to 60 ms, with a proportionately larger number of short delay times. Magic-angle spinning speed was maintained between 3.4 and 3.8 kHz to standardize its contribution to $T_{1\rho}$(C). The initial and final slopes of the ln intensity vs delay time curves were calculated, and their inverses are quoted herein as the short and long component of $T_{1\rho}$(C), respectively.

Results and Discussion

GPC indicated that all samples were high molecular weight polymers. pDNBEM had a peak molecular weight

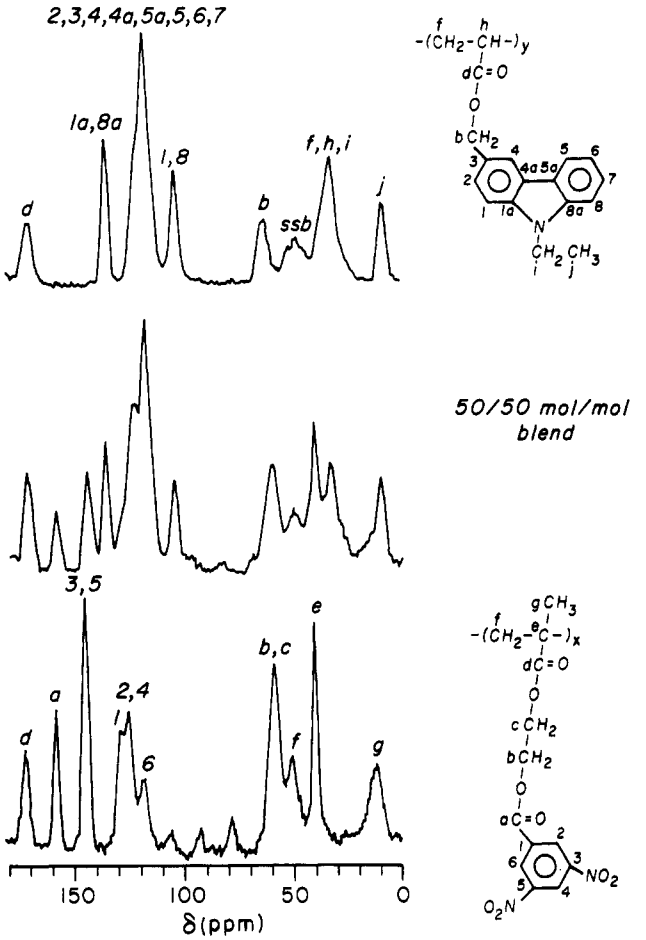

Figure 1. ^{13}C CP/MAS-DD NMR spectra of (top to bottom) pNECMA, a 50/50 mol/mol miscible blend of pNECMA and pDNBEM, and pDNBEM. ssb, spinning side band.

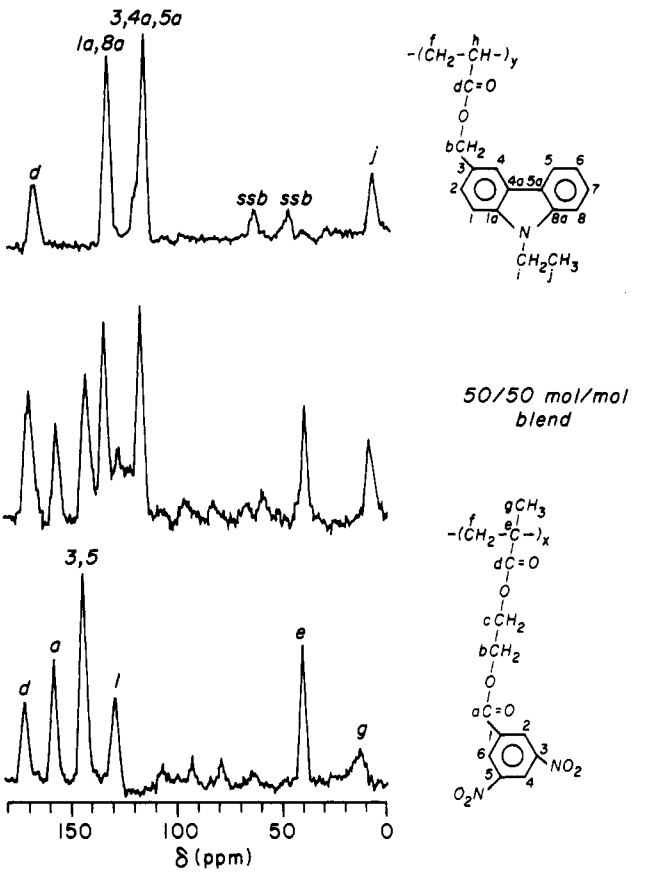

Figure 2. Dipolar-dephased spectra of (top to bottom) pNECMA, a 50/50 mol/mol miscible blend of pNECMA and pDNBEM, and pDNBEM. ssb, spinning side band.

of around 20 000, while that of pNECMM and pNECMA was around 80 000.

Chemical Shift Studies. The ^{13}C CP/MAS-DD spectra of pNECMA, pDNBEM, and a 50/50 mol/mol blend are shown in Figure 1. Figure 2 shows the dipolar-dephased spectra in which only resonances from carbons weakly coupled to protons, that is, nonprotonated or rapidly moving ones, appear. By difference, one obtains Figure 3, which contains the resonances of protonated carbons.

PNECMM and pNECMA exhibit the expected differences between a methacrylate and an acrylate, namely, the disappearance of the main-chain quaternary carbon signal and its replacement by a broader more shielded protonated one. The pNECMA methyl resonance contains only the signal from the CH_3 in the ethyl group on the carbazole nitrogen. It is narrower and more symmetric than the pNECMM methyl resonance, which contains both the *N*-ethyl CH_3 and the α-CH_3, or the pDNBEM methyl resonance from the α-CH_3. Therefore, the α-CH_3 signal in pNECMM and pDNBEM is sensitive to tacticity, as observed in poly(methyl methacrylate) by Schaefer[19] and later deconvoluted by Tonelli et al.[31]

Figures 2 and 3 demonstrate the extent to which it is possible to observe separate resonances for chemically distinct carbons in the homopolymers and the blend. With the exception of the two pendant CH_2 groups, each unique carbon can be resolved in pDNBEM. In pNECMA, the resonances of several aromatic carbons overlap, while upfield the main chain CH and CH_2 and the ethyl CH_2 signals form one broad resonance. In the blend, pD and pA resonances overlap in both the aromatic and main-chain regions. Nevertheless, there is a sufficient number of isolated peaks to perform a chemical shift analysis.

To obtain maximum reproducibility in peak positions, pNECMA, pDNBEM, and 50/50 mol/mol blend, the decomplexed blend, and a repeat of pNECMA, were run consecutively, both conventional and dipolar-dephased spectra, in 1 day, using adamantane as an external reference.

Table I lists the peak positions of all isolated peaks. Some peaks remain unchanged to the level of 0.1 ppm in the homopolymers, the blend, and the decomplexed blend, but show shifts of 1 ppm or more in the miscible blend. Overlapping peaks are not considered here. Still, there is an observable upfield shift in the pDNBEM 1, 3, and 5 aromatic peaks and the benzoyl carbonyl peak in the miscible blend, while the main-chain quaternary peak is unaffected. These shifts are smaller than those observed in a CTC of small-molecule analogues of pNECMM and pDNBEM.[3] They confirm the increase in electron density in the aromatic region of pDNBEM upon CTC formation. The pNECMA peaks are unaffected; either downfield shifts are too small to be observed, or they are compensated for by the aromatic shielding effect in the CTC.[1] The increased reproducibility of the peak positions in these spectra allows the detection of chemical shifts due to the weak CT interactions in this pD/pA pair. Chemical shift effects are very short-range, so the observed differences suggest that the interacting portions of the pD and pA approach each other closely in the blend. The fact that the peak positions in the phase-separated pNECMA/pDNBEM blend are identical to those of the homopolymers confirms that the majority of CT contacts have been broken without any decomposition or other changes to the components.

$T_{1\rho}$(^{13}C) Studies. It is necessary to make a few comments about the data collected and their treatment to calculate $T_{1\rho}$(C). The spectra of the samples examined

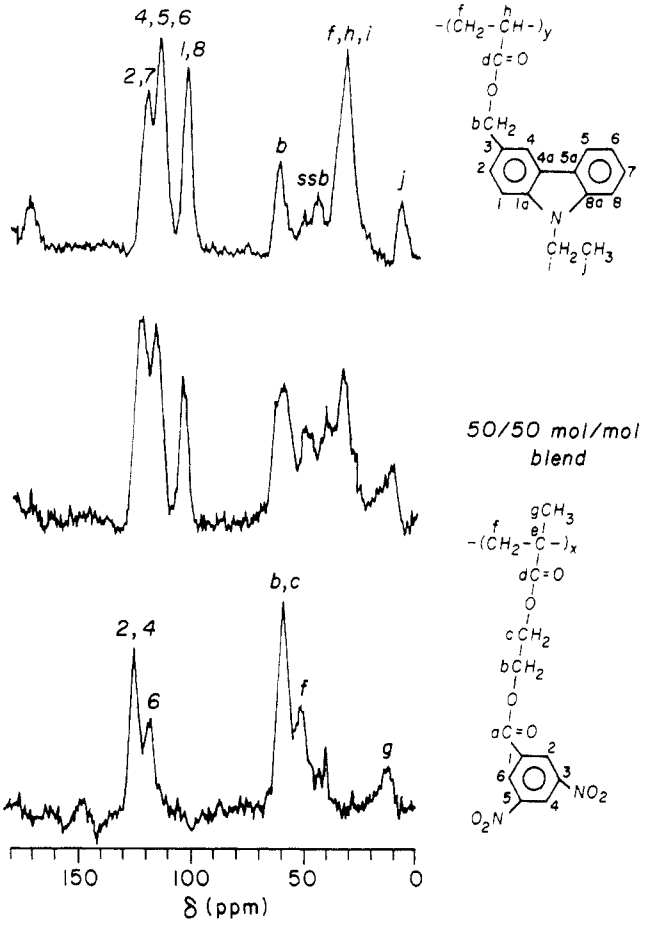

Figure 3. Spectra of protonated carbons in (top to bottom) pNECMA, a 50/50 mol/mol miscible blend of pNECMA and pDNBEM, and pDNBEM. ssb, spinning side band.

Table I
Chemical Shifts (ppm) of Carbons in pNECMA, pDNBEM, and Miscible and Decomplexed 50/50 mol/mol Blends

carbon	pDNBEM	pNECMA	miscible blend (dif[a])	decomplexed blend (dif[a])
a	158.6		157.9 (0.7)	158.5 (0.1)
3, 5	144.9		143.7 (1.2)	144.8 (0.1)
1a, 8a		135.5	135.3 (0.2)	135.5 (0.0)
1	129.5		128.3 (1.2)	129.4 (0.1)
1, 8		104.0	104.2 (0.2)	104.2 (0.2)
e	40.4		40.2 (0.2)	40.3 (0.1)
f, h, j		33.0	33.0 (0.0)	33.1 (−0.1)

[a] The difference in ppm between the shift of the homopolymer and that of the miscible or decomplexed blend.

here are quite crowded; that is, there is not a large region which is free of resonances. This makes determination of the baseline and phasing difficult and is worsened in the blend spectra, which contain resonances from both components. This problem was minimized by increasing the sweep width to provide some resonance-free baseline, spinning as fast as possible to reduce spinning sidebands, and increasing the number of scans to achieve good signal-to-noise ratios. Our experience with a large number of spectra is that peak heights are reproducible to ±5%.

Figure 4 shows the peak height vs delay time data for three different carbons in pDNBEM at 85 °C. Some sets of data cannot be fit by a single exponential. For some resonances, two-component behavior is obvious, but if one component contributes to a very minor degree, or if the two slopes are not different enough, a two-component decay can appear to be exponential. Considering the 5% error on each peak height, some judgement is necessary when fitting the data. In this paper, if a single exponential

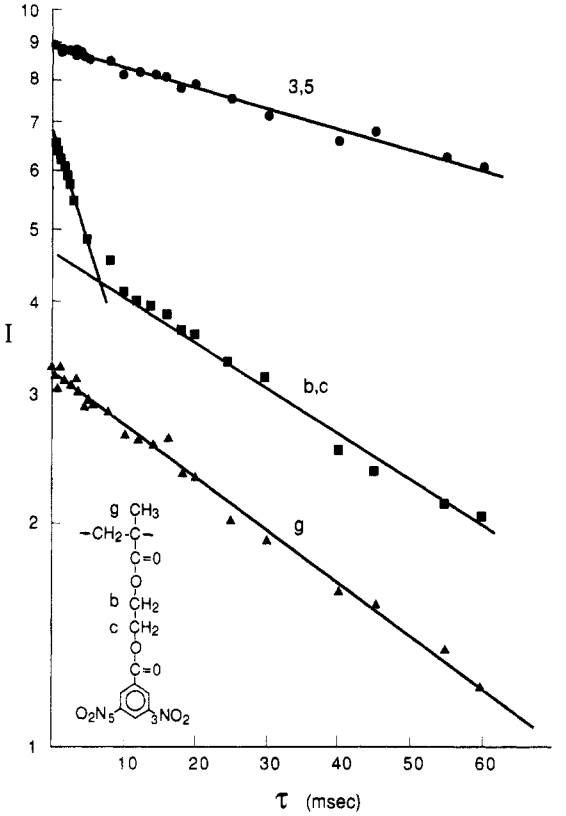

Figure 4. Peak height vs delay time for pDNBEM at 85 °C: Carbons 3, 5 (●), b, c (■), and g (▲).

fits the data to within the expected reproducibility, that is the value used. For ln intensity vs delay time plots which are clearly curved, the initial slope as well as the final slope is reported. Each data set took nearly 48 h to acquire, so the option of sampling at more delay times is impractical since the long-term stability of sample and spectrometer is unclear. As is, we believe that the $T_{1\rho}$(C) values discussed in this paper are accurate to ~10%. Data for every sample were treated the same way so that comparisons between samples and sites in a sample could be made. The letter designation for each carbon site is as in Figures 1–3, and the relevant carbons are shown.

pDNBEM. The variation of $T_{1\rho}$(C) for each resolvable carbon in pDNBEM with temperature is shown in Figures 5–7. The initial and final $T_{1\rho}$(C) for each site and the percent contribution of the slow component (final slope) to the relaxation process are given in Table II. The interpretation of the results for pDNBEM are discussed here in detail, while those for other samples are treated the same way.

Relaxation data can be fit to a single exponential for carbons d, a, 3 and 5, e, and g. Except for the α-CH_3, these are nonprotonated. The relaxation mechanism in the absence of directly bonded protons is not clear, but comparison between similar carbons at different temperatures or sites is possible.

There are several types of comparisons to be made within the data. One is to rank the sites in order of relaxation rate. Carbon d relaxes most slowly, followed by a, 3 and 5, e, g, 1, 2 and 6 = 4, b and c, and f. The slowest relaxing moieties are the carbonyl carbons, the nitro carbons, and the main-chain quaternary carbon. Their slow relaxation is surely due in part to the lack of directly bonded protons. The α-CH_3 group with three directly bonded protons relaxes more slowly than the fast component of the aromatic protons, and the pendant and main-chain CH_2 groups relax most quickly. This sequence is related to the

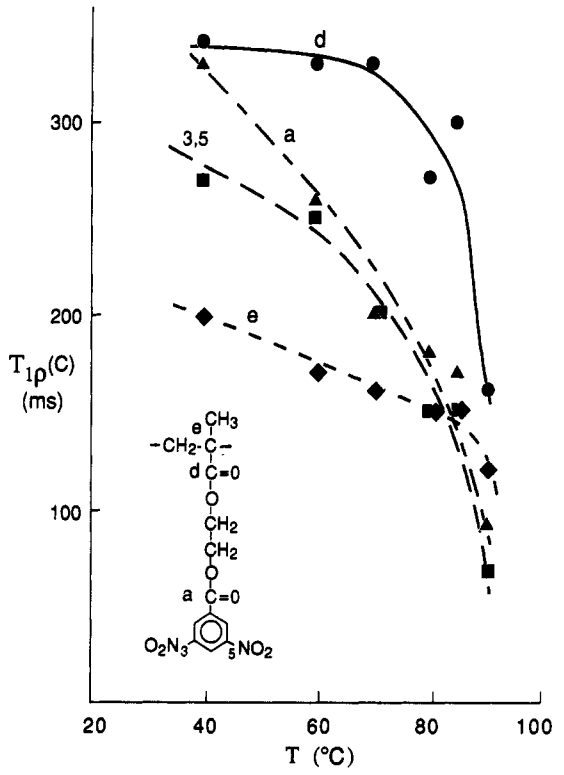

Figure 5. $T_{1\rho}$(C) vs temperature for pDNBEM: Carbons d (●), a (▲), 3, 5 (■), and e (◆).

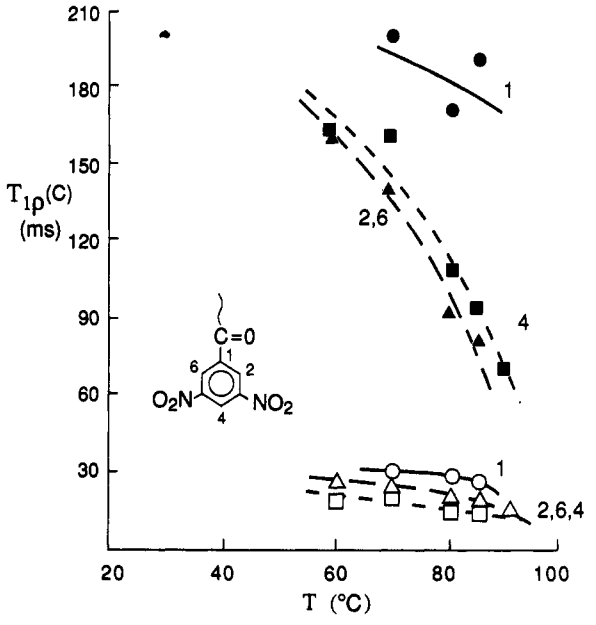

Figure 6. $T_{1\rho}$(C) vs temperature for pDNBEM: Carbons 1 long (●) and short (○) components; 2, 6 long (▲) and short (△) components; and 4 long (■) and short (□) components.

spectral density at 64 kHz. The aromatic groups, and especially the CH_2 groups, have a larger component of motion at this frequency than the CH_3 group. Since the CH_3 group is expected to be undergoing fast free rotation, it may relax more slowly than the CH_2 because it is moving faster than 64 kHz.

Increasing the temperature increases the mobility at all sites in the sample. Determining the effect of increased mobility on $T_{1\rho}$(C) by variable-temperature studies enables one to discover which side of the $T_{1\rho}$(C) minimum different carbons are on and confirms the interpretation of $T_{1\rho}$(C) as a motional parameter, because spin–spin interactions should decrease as motion increases. The T_g of both pDNBEM and pNECMA is 104 °C, so with high spinning

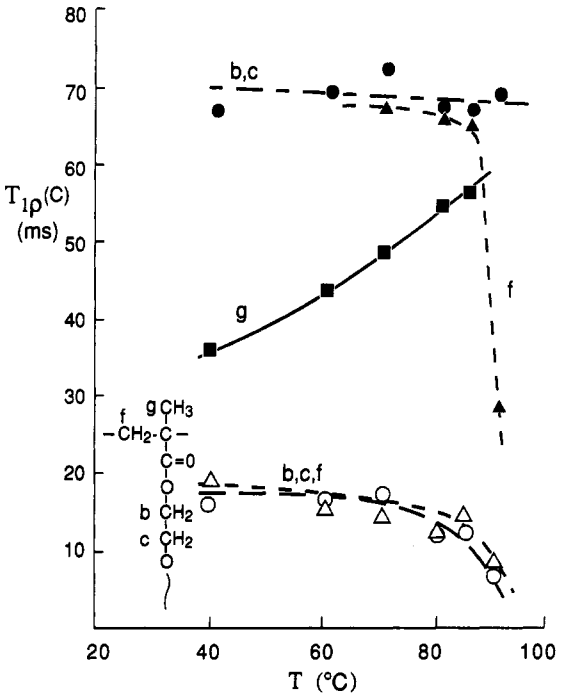

Figure 7. $T_{1\rho}$(C) vs temperature for pDNBEM: Carbons g (■); b, c long (●) and short (○) components; and f long (▲) and short (△) components.

speed and long acquisition times we did not run experiments above 90 °C. At that point the polymers have softened considerably, and motions important in T_g should be beginning to contribute to relaxation.

Figures 5–7 show that different carbons have different patterns for changes in $T_{1\rho}$(C) with temperature. The α-CH_3 carbon's relaxation rate decreases as the temperature is increased. This confirms that, even below T_g, motion at this site is faster than 64 kHz, so increasing mobility decreases the relaxation rate. All other sites must be on the low-temperature side of the $T_{1\rho}$(C) minimum, since increasing the temperature makes them relax faster. Relaxation at these sites is best discussed for groups of carbons which form different parts of the repeat unit. $T_{1\rho}$(C) for the benzoyl C=O, the nitro carbons, and the slow component of the protonated aromatic carbon relaxation all decrease steadily as the temperature increases from 40 to 90 °C. The proportion of the slow component remains constant until around 80 °C and then it drops suddenly. The fast component of the aromatic carbon relaxation decreases only slightly with increasing temperature. $T_{1\rho}$(C)'s for the methacrylate C=O, and both the fast and slow components of the main-chain and pendant CH_2 carbons, do not change much until the temperature reaches 80–90 °C, when they drop quickly. For the main-chain carbons only, the percentage of fast component increases steadily with temperature, although the magnitudes of the fast and slow components do not.

The observed trends in $T_{1\rho}$(C) suggest that below T_g the aromatic groups are involved in some sort of mid-kilohertz motion which increases in frequency or amplitude steadily as the temperature is raised. Using ^{13}C solid-state NMR, Schaefer et al. concluded that ring flips or small-angle oscillations are an important relaxation mechanism for polystyrenes.[20] Both the slow and fast components of the main-chain and pendant CH_2 groups' relaxation appear to be related to long-range cooperative motions, since it is only near T_g that a large increase in relaxation rate is observed. The onset of long-range motions may also be responsible for the increase in the

Table II
Variation of $T_{1\rho}$(C) Parameters for pDNBEM with Temperature

carbon	$T_{1\rho}$,[a] ms	temp, °C					
		40	60	70	80	85	90
d	-	340	330	330	270	300	150
a	-	330	260	200	180	170	92
3, 5	-	270	250	200	150	150	66
1	s (%)	160	170	200 (89)	170 (89)	190 (89)	75
	f			30	29	25	
2, 6	s (%)	76	160 (74)	140 (73)	91 (74)	81 (78)	
	f		27	25	19	19	14
4	s (%)	89	160 (75)	160 (75)	110 (75)	93 (74)	70 (57)
	f		20	24	17	15	15
b, c	s (%)	67 (78)	70 (77)	73 (71)	68 (66)	68 (70)	70 (29)
	f	16	17	18	12	13	7
f	s (%)	57 (85)	50 (73)	68 (64)	67 (62)	66 (57)	29 (50)
	f	19	16	15	12	15	9
e	-	200	170	160	150	150	12
g	-	36	44	49	55	57	51

[a] This column specifies whether the data were fit with one or more exponentials. "-" indicates that the data were fit by one exponential and that is the $T_{1\rho}$(C) quoted. If more than one exponential was necessary, "s" refers to the slow component with "%" being its contribution to the overall relaxation and "f" refers to the fast component (initial slope to ~2 ms).

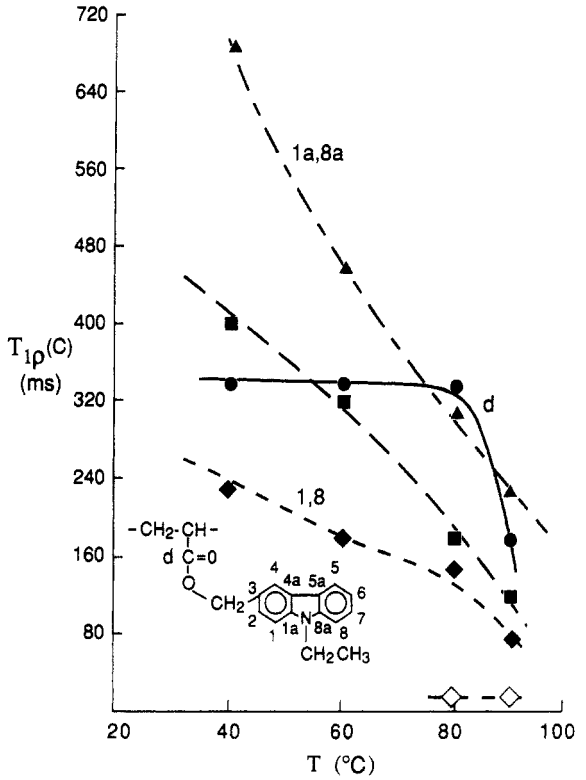

Figure 8. $T_{1\rho}$(C) vs temperature for pNECMA: Carbons d (●); 1a, 8a (▲); 2, 3, 4, 4a, 5a, 5, 6, 7 (■); and 1, 8 long (◆) and short (◇) components.

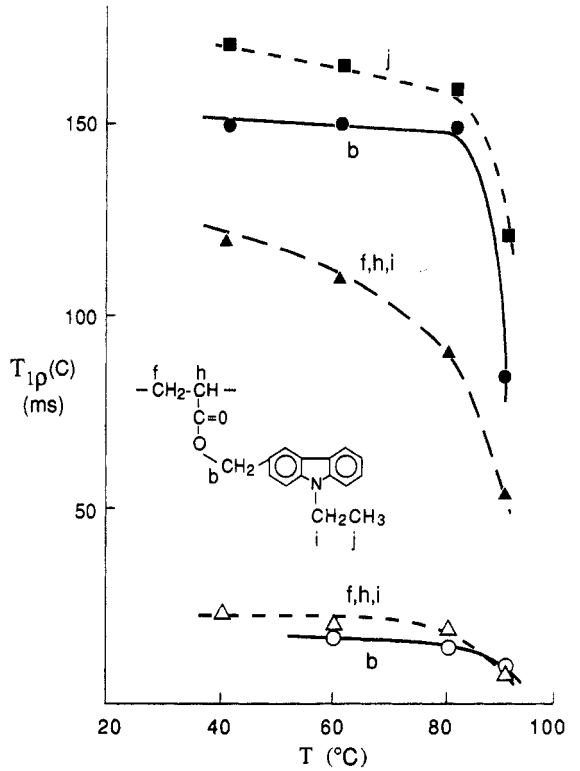

Figure 9. $T_{1\rho}$(C) vs temperature for pNECMA: Carbons j (■); b long (●) and short (○) components; and f, h, i long (▲) and short (△) components.

contribution of the fast component to overall relaxation of aromatic carbons and pendant CH_2 groups at 90 °C. This is reasonable because the side groups would be pulled along with the main chain as it begins to move. The increase in proportion of the fast component of main-chain carbons with temperature may indicate the presence of small-angle wiggles in the main chain which take place in more sites with increasing temperature but can never really have significant amplitude because of steric restrictions. The onset of long-range motion at T_g results in fast relaxation at these sites.

pNECMA and pNECMM. Figures 8 and 9 show the variation in $T_{1\rho}$(C) for the resolvable carbons in pNECMA, and Table III lists the $T_{1\rho}$(C) values. Except for the acrylate C=O carbon, carbons in pNECMA relax more slowly than similar carbons in pDNBEM at the same temperature. PNECMA and pDNBEM have the same T_g, so we expected similar spectral densities at 64 kHz in both at a given temperature. The slower relaxation of the aromatic carbons in pNECMA may be due to the greater bulk of the carbazole group. Even though the onset of long-range motion occurs at the same temperature in both polymers, the sub-T_g motions of the pendant group appear to be less important in pNECMA.

The relaxation time constants from pNECMA resonances increase in the following order: f, h, j; b; i; 1, 8; d; 2, 3, 4, 4a, 5a, 5, 6, 7; and 1a, 8a. The two sets of CH_2 groups relax fastest, as was observed in pDNBEM. This is partly because of the attached protons, but also reflects a larger spectral density at 64 kHz for these sites, since the faster moving CH_3 groups has more protons but relaxes more slowly than the CH_2. The CH_3 of pNECMA is located on the *N*-ethyl group, and its $T_{1\rho}$(C) is relatively insensitive to temperature, although it does finally decrease at 90 °C.

Table III
Variation of $T_{1\rho}$(C) Parameters for pNECMA and pNECMM with Temperature

		temp, °C					
		pNECMA				pNECMM	
carbon	$T_{1\rho}$,[a] ms	40	60	80	90	70	85
d	-	340	340	340	180	560	550
1a, 8a	-	690	460	310	230	460	390
2, 3, 4, 4a 5a, 5, 6, 7	-	400	320	180	120	280	220
1, 8	s (%)	230	180	150 (83)	80 (83)	310 (86)	184 (84)
	f			16	15	60	21
b	s (%)	150	150 (86)	150 (83)	85 (77)	190 (86)	210 (83)
	f		18	16	11	42	47
e	-		-	-	-	200	140
f, h, i	s (%)	120 (91)	110 (84)	91 (79)	55 (73)	-	-
	f	24	21	21	9		
i	s (%)	-	-	-	-	130 (84)	99 (79)
	f	-	-	-	-	50	30
j	-	170	165	160	120		
g, j	-	-	-	-	-	120	110

[a] See Table II.

The relaxation rate of the aromatic carbons is slow but increases steadily with temperature, so there is some sub-T_g motion in pNECMA, but its amplitude or frequency may be less than in pDNBEM. As in pDNBEM, the main-chain and pendant CH_2 carbon relaxation rates experience a drastic drop at 90 °C, presumably because the polymer is approaching its T_g.

The relaxation rates for the resolvable carbons in pNECMM show trends similar to those in pNECMA, but the relaxation rates at all sites are slower in pNECMM than in pNECMA at a given temperature. No drastic increase in the relaxation rate of pNECMM is observed at 80–90 °C. This can be accounted for by the presence of the α-CH_3 group in pNECMM, which has the effect of hindering backbone motion and raising the T_g by 35 °C. Therefore, when we perform a $T_{1\rho}$(C) experiment at 90 °C, we are only 14 °C below the T_g of pNECMA, but 50 °C below the T_g of pNECMM. We should not see a large change in the relaxation rate of the main-chain carbons of pNECMM until a higher temperature. Faster relaxation of the aromatic carbons with increasing temperature is observed in pNECMM, however, so there is still increasing sub-T_g motion at this site with rising temperature. The $T_{1\rho}$(C) of the methyl peak in pNECMM does not change as the temperature is increased. Since this peak contains overlapping resonances for the α-CH_3 and the N-ethyl CH_3, it is possible that the α-CH_3 is moving quite quickly, while the other methyl group has some other temperature dependence for $T_{1\rho}$(C), but we could not separate these peaks to confirm this.

pD/pA Blends. Although measurements were performed on pNECMM/pDNBEM blends also, this discussion focuses on the data for pNECMA/pDNBEM samples. There are several reasons for this: the number of temperatures used for the pNECMM-containing blends was smaller; the slower relaxation of pNECMM required a greater reproducibility of peak heights to fit the data accurately; pNECMA, pDNBEM, and the decomplexed blend all have a T_g of 104 °C, and the miscible blend has a T_g of 119 °C compared to 136 °C for the pNECMM-containing blend, so we were able to approach T_g more closely without sample decomposition in pNECMA-containing samples. The results obtained for the pNECMM/pDNBEM blends are consistent with those presented here for the pNECMA/pDNBEM samples.

Figure 1 shows that the spectra of pNECMA and pDNBEM overlap considerably. While the chemical shift analysis was facilitated by the spectral editing provided by dipolar dephasing, this is not the case with the $T_{1\rho}$(C) data. There was more scatter in the blend data, possibly reflecting increased molecular-level heterogeneity of chemical environments compared to the homopolymers. Any $T_{1\rho}$(C) within 10% of the homopolymer values is considered unchanged. The only peaks in which there is not significant overlap of pNECMA and pDNBEM resonances are those of the pDNBEM benzoyl C=O carbon, the aromatic group nitro carbons, and the main-chain quaternary carbon; for pNECMA, the carbazole 1, 8 and 1a, 8a carbon signals and the f, h, i peak are resolvable.

In general, little change in the $T_{1\rho}$(C) values from the homopolymers to the blend or decomplexed blend was observed. In blend peaks made up of overlapping homopolymer resonances, the relaxation rate fell somewhere between those of the components. Of the isolated peaks, the pDNBEM main-chain quaternary signal and all the pNECMA signals yielded $T_{1\rho}$(C) values within experimental error of the homopolymer values.

There appear to be some differences in the $T_{1\rho}$(C) trends for the benzoyl C=O and aromatic nitro carbons in pDNBEM and in the blends. Figures 10 and 11 show $T_{1\rho}$(C) obtained for pure pDNBEM and pDNBEM in the miscible and decomplexed blends. At 60 °C, these carbons have the same $T_{1\rho}$(C) in the homopolymer and the blends. As the temperature is increased, the $T_{1\rho}$(C) of the homopolymer carbons decreases quickly, the decomplexed blend more slowly, and the miscible blend hardly at all. The increase in relaxation rates at these sites with temperature in the homopolymer was rationalized above as reflecting aromatic group motion which increases in amplitude or frequency with temperature, followed by the onset of long-range motions above 90 °C. It appears that in the miscible blend some component of these motions is damped by CTC formation. This is consistent with the higher T_g of the blend, which means that at 90 °C we are still 30 °C away from T_g, compared to 14 °C away for pDNBEM. The slight decrease in relaxation rate even in the decomplexed blend may imply that there is some damping of the short-range group motions as well, even though the T_g has returned to the homopolymer value. Alternatively, it may reflect residual CT complexation at the interface of pD and pA phases which effectively gives the interfacial region a different T_g than the interior of each phase. Residual CT complexation at the interface has been suggested as the origin of the reduced $T_{1\rho}$(H) of

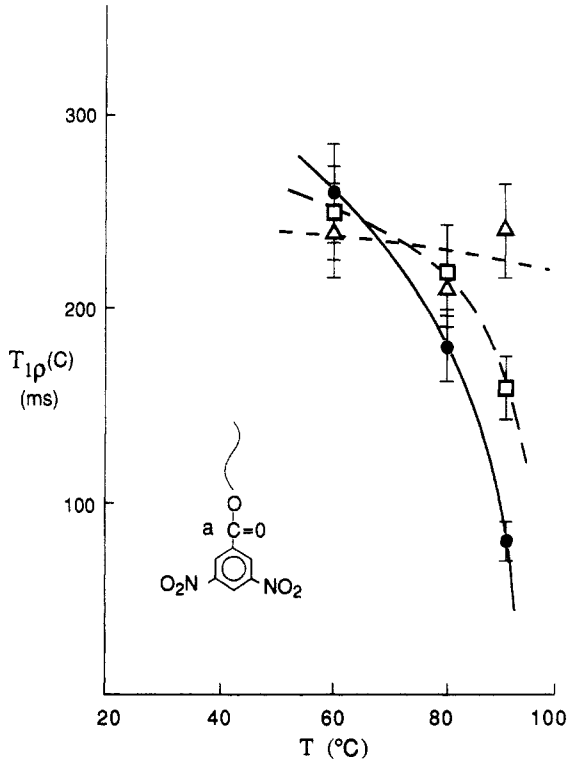

Figure 10. $T_{1\rho}$(C) vs temperature for the pDNBEM benzoyl C=O carbon in pDNBEM (●) and miscible (△) and decomplexed (□) 50/50 mol/mol pNECMA/pDNBEM blends.

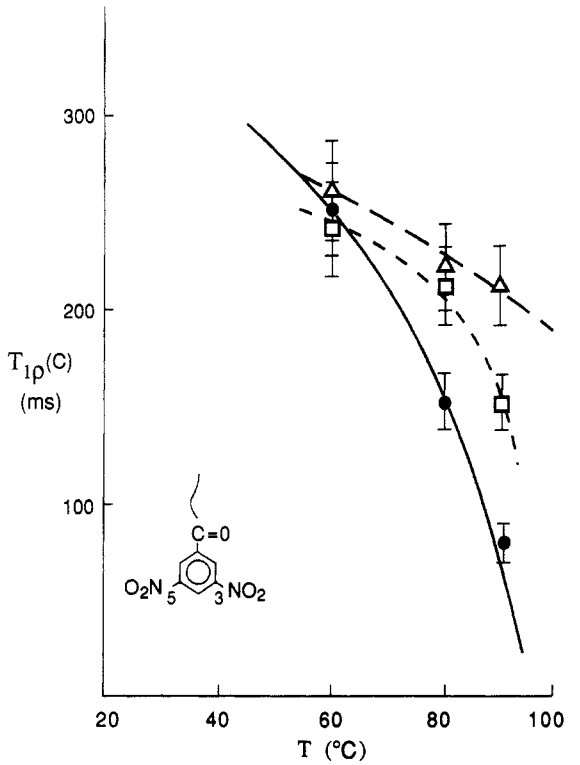

Figure 11. $T_{1\rho}$(C) vs temperature for the pDNBEM nitro carbons in pDNBEM (●) and miscible (△) and decomplexed (□) 50/50 mol/mol pNECMA/pDNBEM blends.

the donor component in pDNBEM/pNECMA blends.[4]

The resonances which appear to undergo changes in $T_{1\rho}$(C) on blending are the ones that were shifted upfield in the chemical shift studies, that is, the pDNBEM benzoyl C=O and nitro carbons. The resonance of the other shifted carbon, the aromatic 1-carbon, is buried in the composite pD–pA aromatic resonance.

General Discussion. By optimizing acquisition conditions, we have obtained spectra in which the reproducibility of the peak positions is sufficient to detect differences between the chemical shift of some pDNBEM resonances in the homopolymer and in a miscible blend with pNECMA. The observed changes show the same trend as that observed in CTCs of small-molecule models and are consistent with the transfer of electron density from pNECMA to the aromatic region of pDNBEM. The chemical shifts of pDNBEM and pNECMA in the same blend after phase separation are indistingushable from those of the pure homopolymers.

We determined $T_{1\rho}$(C) for all resolvable carbons of pDNBEM, pNECMA, and pNECMM at various temperatures. By observing the effect on $T_{1\rho}$(C) of increasing the sample mobility by heating, we concluded that all carbons with the exception of the α-CH_3 are on the low-temperature side of the $T_{1\rho}$(C) minimum at the temperatures studied. There is some sub-T_g motion of the aromatic groups which increases steadily in amplitude or frequency as the temperature is raised. The relaxation rate of the main-chain carbons and pendant CH_2 groups does not increase significantly until nearly 90 °C, close to the onset of long-range cooperative motions involved in the glass transition. Sub-T_g relaxation in pNECMA is less important than in pDNBEM, perhaps due to the large free volume necessary for even small-angle displacements of the bulky carbazole moiety. The slow relaxation of pNECMM relative to pNECMA was attributed to the presence of the α-CH_3 group, which hinders main-chain motion and increases T_g.

Analysis of $T_{1\rho}$(C) in the one- and two-phase pNECMA/pDNBEM blends is hampered by substantial overlap between the component spectra. Most isolated signals in the blends yield $T_{1\rho}$(C) values unchanged from those in the homopolymers. At 90 °C, the pDNBEM benzoyl C=O carbon and the nitro carbons appear to relax more slowly in the decomplexed blend, and especially in the miscible blend, than in pure pDNBEM. This implies some reduction in motion at the sites of maximum electron transfer in the CTC. However, we previously observed large increases in the rate of proton spin diffusion on blending pNECMA and pDNBEM.[4] Because these carbons are on the low-temperature side of the $T_{1\rho}$(C) minimum, slowing down of motion in the blends should reduce the relaxation rate, and in any case, the small motional changes proposed here do not account for the substantial enhancement in spin diffusion we observed. This is consistent with our prior interpretation of $T_{1\rho}$(H) as a measure of interproton distance, and not of motion at 64 kHz, in these samples.

Conclusions

Chemical shift changes in pDNBEM on blending with pNECMA suggest a close approach of the aromatic groups of pD and pA in polymer CTC complexes. By measuring $T_{1\rho}$(C) at various temperatures, we were able to show its usefulness as a motional parameter in these samples and demonstrate that different modes of motion contribute to relaxation in the main-chain and pendant groups of pDNBEM, pNECMA, and pNECMM. No large changes in mobility are observed on blending, but there may be some damping of motion at the sites where chemical shift changes were detected.

Acknowledgment. A.S. is grateful to the Ontario Center for Materials Research for financial support. We thank the Natural Science and Engineering Research Council of Canada and Queen's University for funding.

References and Notes

(1) Natansohn, A.; Simmons, A. *Macromolecules* **1989**, *22*, 4426.
(2) Simmons, A.; Natansohn, A. *Macromolecules* **1990**, *23*, 5127.
(3) Simmons, A.; Natansohn, A. *Macromolecules* **1991**, *24*, 3651.
(4) Simmons, A.; Natansohn, A. *Macromolecules* **1992**, *25*, 1272.
(5) Rodriguez-Parada, J. M.; Percec, V. *Macromolecules* **1986**, *19*, 55.
(6) Grobelny, J.; Rice, D. M.; Karasz, F. E.; MacKnight, W. *Polym. Commun.* **1990**, *31*, 87.
(7) Grobelny, J.; Rice, D. M.; Karasz, F. E.; MacKnight, W. J. *Macromolecules* **1990**, *23*, 2139.
(8) Zhang, X.; Takegoshi, K.; Hikichi, K. *Polym. J.* **1991**, *23*, 87.
(9) Qin, C.; Pires, A. T. N.; Belfiore, L. A. *Polym. Commun.* **1990**, *31*, 177.
(10) Qin, C.; Pires, A. T. N.; Belfiore, L. A. *Macromolecules* **1991**, *24*, 666.
(11) Zhang, X.; Takegoshi, K.; Hikichi, K. *Macromolecules* **1991**, *24*, 5756.
(12) Masson, J. F.; Manley, R. S. J.; *Macromolecules* **1991**, *24*, 5914.
(13) Natansohn, A. L. *Polym. Bull.* **1983**, *9*, 67.
(14) Natansohn, A. *J. Polym. Sci., Polym. Chem. Ed.* **1984**, *22*, 3161.
(15) Natansohn, A. *Macromolecules* **1991**, *24*, 1662.
(16) Uryu, T.; Furuichi, T.; Oshima, R. *Macromolecules* **1988**, *21*, 1890.
(17) Schaefer, J.; Sefcik, M. D.; Stejskal, E. O.; McKay, R. A. *Macromolecules* **1984**, *17*, 1118.
(18) Schaefer, J.; Stejskal, E. O.; Steger, T. R.; Sefcik, M. D.;. McKay, R. A. *Macromolecules* **1980**, *13*, 1121.
(19) Schaefer, J.; Stejskal, E. O.; Buchdahl, R. *Macromolecules* **1977**, *10*, 384.
(20) Schaefer, J.; Sefcik, M. D.; Stejskal, E. O.; McKay, R. A.; Dixon, W. T.; Cais, R. E. *Macromolecules* **1984**, *17*, 1107.
(21) Sefcik, M. D.; Schaefer, J.; Stejskal, E. O.; McKay, R. A. *Macromolecules* **1980**, *13*, 1132.
(22) Jelinski, L. W.; Dumais, J. J.; Watnick, P. I.; Engel, A. K.; Sefcik, M. D. *Macromolecules* **1983**, *16*, 409.
(23) Allen, P. E. M.; Simon, G. P.; Williams, D. R. G.; Williams, E. H. *Macromolecules* **1989**, *22*, 809.
(24) Hatfield, G.; Aharoni, S. M. *Macromolecules* **1989**, *22*, 3807.
(25) Curran, S. A.; LaClair, C. D.; Aharoni, S. M. *Macromolecules* **1991**, *24*, 5903.
(26) Schneider, H. A.; Cantow, H.-J.; Percec, V. *Polym. Bull.* **1982**, *6*, 617.
(27) Simmons, A.; Natansohn, A. *Polym. Mater. Sci. Eng.* **1991**, *65*, 158.
(28) Simionescu, C. I.; Percec, V. *J. Polym. Sci., Polym. Chem. Ed.* **1979**, *17*, 2287.
(29) Simionescu, C. I.; Percec, V.; Natansohn, A. *Polym. Bull.* **1980**, *3*, 535.
(30) Opella, S. J.; Frey, M. H. *J. Am. Chem. Soc.* **1979**, *101*, 5854.
(31) Tanaka, H.; Gomez, M. A.; Tonelli, A. E. *Macromolecules* **1988**, *21*, 2934.

Registry No. pDNBEM (homopolymer), 82008-07-9; pNECMM (homopolymer), 67549-45-5; pNECMA (homopolymer), 71356-19-9.